

- ron Letters 1980, 21, 4091.
- Yoh, S.-D.; Kweon, J. M.; Byeon, S. I.; Fujio, M.; Mishima, M.; Tsuno, Y. *Bull. Korean Chem. Soc.* 1996, 17(3), 228.
 - (a) Yukawa, Y.; Tsuno, Y. *Bull. Chem. Soc. Jpn.* 1959, 32, 971. (b) Yukawa, Y.; Tsuno, Y.; Sawada, M. *Bull. Chem. Soc. Jpn.* 1966, 39, 2274.
 - Liu, K. T.; Kuo, M. Y.; Sheu, C. F. *J. Am. Chem. Soc.* 1982, 104, 211.
 - Grunwald, E.; Winstein, S. *J. Am. Chem. Soc.* 1948, 70, 846.
 - Winstein, S.; Grunwald, E.; Jones, H. W. *J. Am. Chem. Soc.* 1951, 73, 2770.
 - (a) Fujio, M.; Goto, M.; Funatsu, K.; Yoshino, T.; Tsuno, Y. *Mem. Fac. Sci. Kyushu Univ. Ser. C.* 1990, 17(2), 255. (b) Fujio, M.; Goto, M.; Funatsu, K.; Yoshino, T.; Saeki, Y.; Yatsugi, K.; Tsuno, Y. *Bull. Chem. Soc. Jpn.* 1992, 65, 46. (c) Kevill, D. N.; Ismail, N. H.; D'Souza, M. J. *J. Org. Chem.* 1994, 59, 6303. (d) Bently, T. W.; Koo, I. S.; Norman, S. J. *J. Org. Chem.* 1991, 56, 1604.
 - (a) Schadt, F. L.; Bently, T. W.; Schleyer, P. v. R. *J. Am. Chem. Soc.* 1976, 98, 7667. (b) Bently, T. W.; Schleyer, P. v. R. *Adv. Phys. Org. Chem.* 1977, 14, 1. (c) Kevill, D. N.; Anderson, S. W. *J. Org. Chem.* 1991, 56, 1845.
 - (a) Dau-Schmidt, J. P.; Llewellyn, G. *Prog. Phys. Org. Chem.* 1991, 17, 121. (b) Fainberg, A. H.; Winstein, S. *J. Am. Chem. Soc.* 1957, 79, 1597, 1602. (c) Fujio, M.; Tomita, N.; Tsuno, Y.; Kobayashi, S.; Taniguchi, H.; Kaspri, J.; Rappoport, Z. *Tetrahedron Lett.* 1992, 33, 1309. (d) Bently, T. W.; Dau-Schmidt, J. P.; Llewellyn, G.; Mayr, H. *J. Org. Chem.* 1992, 57, 1791.
 - Liu, K. T.; Sheu, H. C. *J. Org. Chem.* 1991, 56, 3021.
 - (a) Bently, T. W.; Carter, G. E. *J. Am. Chem. Soc.* 1982, 104, 5471. (b) Bently, T. W.; Roberts, K. *J. Chem. Soc., Perkin Trans. 2.* 1989, 1055.
 - Fujio, M.; Susuki, T.; Goto, N.; Tsuji, Y.; Yatsugi, K.; Saeki, Y.; Kim, S. H.; Tsuno, Y. *Bull. Chem. Soc. Jpn.* 1994, 67, 2233.
 - (a) Fujio, M.; Saeki, Y.; Nakamoto, K.; Yatsugi, K.; Goto, N.; Kim, S. H.; Tsuji, Y.; Rappoport, Z.; Tsuno, Y. *Bull. Chem. Soc. Jpn.* 1995, 68, 2603. (b) Fujio, M.; Susuki, T.; Yatsugi, K.; Saeki, Y.; Goto, N.; Kim, S. H.; Tsuji, Y.; Rappoport, Z.; Tsuno, Y. *Bull. Chem. Soc. Jpn.* 1995, 68, 2619.
 - (a) Kevill, D. N.; Aderson, S. W. *J. Am. Chem. Soc.* 1986, 108, 1579. (b) Kevill, D. N.; D'Souza, M. J. *J. Chem. Soc., Perkin. Trans. 2.* 1995, 973. (c) Kevill, D. N.; Bahnke, J. *J. Chem. Soc., Perkin. Trans. 2.* 1995, 1777.
 - Perrin, D. N.; Armarego, W. L. F. *Purification of Laboratory Chemicals*, 3rd ed.; Pergamon press: New York, 1988.

Tetrathiafulvalene (TTF) Charge Transfer Compounds with Some Heavier Transition Metal (Au, Pt, Ir, Os) Chlorides

Chan-Kyou Jeong, Young-Inn Kim*, and Sung-Nak Choi†

*Department of Chemical Education, The Pusan National University, Pusan 609-735, Korea

†Department of Chemistry, The Pusan National University, Pusan 609-735, Korea

Received August 14, 1996

The charge transfer compounds of tetrathiafulvalene (TTF) with the general formula of $(\text{TTF})_n\text{MCl}_n$ ($\text{M}=\text{Au, Pt, Ir, Os}$) were prepared by the direct reaction using excess $\text{HAuCl}_4 \cdot 3\text{H}_2\text{O}$, $\text{H}_2\text{PtCl}_6 \cdot x\text{H}_2\text{O}$, $\text{H}_2\text{IrCl}_6 \cdot x\text{H}_2\text{O}$ and H_2OsCl_6 respectively. The powdered electrical conductivities (σ_p) at room temperature are given as follows; $(\text{TTF})_3\text{AuCl}_2$, 4.53×10^{-3} ; $(\text{TTF})_{3.5}\text{AuCl}_2$, 6.37×10^{-3} ; $(\text{TTF})_3\text{PtCl}_4$, 5.51×10^{-4} ; $(\text{TTF})_2\text{IrCl}_4$, 2.40×10^{-5} ; $(\text{TTF})\text{OsCl}_4 \cdot 1/2\text{C}_2\text{H}_5\text{OH}$, $4.46 \times 10^{-7} \text{ Scm}^{-1}$. Magnetic susceptibility, electronic (UV-Vis.), vibrational (IR) and EPR spectroscopic evidences indicate that there is incomplete charge transfer from the TTF donor to gold, platinum, and iridium respectively, and that there is essentially complete charge transfer to osmium, thereby resulting a relatively low electrical conductivity in osmium compound. The EPR and magnetic susceptibility data reflect that the metals are in diamagnetic Au(I), Pt(II), Ir(III), and Os(II) oxidation states, and the odd electrons are extensively delocalized over the TTF lattices in each compound.

Introduction

Tetrathiafulvalene (TTF) has been used as an electron donor to form highly conductive charge transfer compounds. The structural and electronic properties of TTF are considered to be important determinants of electrical-transport properties in crystals of conductive materials. The most famous

compound, TTF-TCNQ (TCNQ=tetracyanoquinodimethane) exhibits highly metallic conductivity which rises to almost 10^4 Scm^{-1} at around 55 K.¹⁻³ It has been concluded that compounds with high electrical conductivities should be formed from donor-acceptor molecules that are in partial oxidation states with uniform structures containing segregated stacks of the constituent molecules.^{1,4} We have prepared^{5,6}

a series of TTF charge transfer compounds with some transition metal complexes to develop conductive materials, and pointed that the oxidation state of TTF plays an important role to exhibit high electrical conductivity. For example, the powdered electrical conductivity of partially oxidized TTF salts with iron compounds is five orders of magnitude greater than those of completely oxidized TTF simple salts.⁵ This result indicates that partial electron transfer is among the factors that lead to high electrical conductivity.

In this work, as the extension of the study, we prepared TTF compounds with some hydrogen transition metal (gold, platinum, iridium, and osmium) chlorides instead of using simple metal chlorides complexes. Therefore we investigated whether the hydrogen is substituted with TTF to form a simple salt or the partial electron transfer is occurred during the reaction. The compounds were characterized using electrical conductivity and magnetic susceptibility measurements, and by EPR, electronic, vibrational spectroscopy, and electrochemical method.

Experimental

All chemicals used for preparations were treated under argon atmosphere in a glove box. $(\text{TTF})_3\text{AuCl}_2$ was prepared by the direct reaction of TTF and $\text{HAuCl}_4 \cdot 3\text{H}_2\text{O}$. $\text{HAuCl}_4 \cdot 3\text{H}_2\text{O}$ (0.3 mmol) was dissolved in 10 mL of a mixture of deoxygenated absolute ethanol and triethylorthoformate (5 : 1). The $\text{HAuCl}_4 \cdot 3\text{H}_2\text{O}$ solution was added dropwise to excess TTF (1.0 mmol) dissolved in 25 mL of the same solvent with constant stirring under an argon atmosphere. The solution was changed to purple immediately. The reaction mixture was stirred for *ca.* 2 hours, and then refrigerated overnight. The resultant purple colored precipitates were collected by filtration and washed several times with absolute ethanol. The microcrystalline precipitates were dried in vacuum dry oven at room temperature. $(\text{TTF})_{3.5}\text{AuCl}_2$ was prepared by the similar method using CH_2Cl_2 solvent. $(\text{TTF})_3\text{PtCl}_4$, $(\text{TTF})_2\text{IrCl}_4$ and $(\text{TTF})\text{OsCl}_4 \cdot 1/2\text{C}_2\text{H}_5\text{OH}$ were also formed by the similar method using $\text{H}_2\text{PtCl}_6 \cdot x\text{H}_2\text{O}$, $\text{H}_2\text{IrCl}_6 \cdot x\text{H}_2\text{O}$ and H_2OsCl_6 in ethanol, respectively.

Elemental analysis were performed by Korean Basic Science Center (E.A. 1108 Elemental Analyzer), which satisfactory results were obtained for all compounds. The analytical data of these compounds are given as follows.

Anal. Calc. for $(\text{TTF})_3\text{AuCl}_2$: C, 24.54; H, 1.37. Found: C, 24.68; H, 1.45. Calc. for $(\text{TTF})_{3.5}\text{AuCl}_2$: C, 25.66; H, 1.44. Found: C, 25.58; H, 1.46. Calc. for $(\text{TTF})_3\text{PtCl}_4$: C, 22.76; H, 1.27. Found: C, 22.88; H, 1.28. Calc. for $(\text{TTF})_2\text{IrCl}_4$: C, 19.40; H, 1.09. Found: C, 19.31; H, 1.28. Calc. for $(\text{TTF})\text{OsCl}_4 \cdot 1/2\text{C}_2\text{H}_5\text{OH}$: C, 15.03; H, 1.26. Found: C, 14.99; H, 1.37.

The room temperature powdered electrical conductivities were determined by compressing the bulk sample between two graphite rods (5 mm in diameter) surrounded by a glass tube sheath.⁷ These determinations were made with a EG & G Model 362 scanning potentiostat in a two electrode configuration at room temperature. EPR spectral measurements were made on powdered samples at 77 K using a ESP-300S EPR spectrometer at X-band frequency. The field modulation frequency was 100 kHz. Magnetic susceptibility data were collected from 5 K to 300 K using MPMS7 (Magnetic Property Measurement System) of U.S.A. Quantum Design by

SQUID method. The data were collected for temperature independent paramagnetism and for the diamagnetism of the constituent atoms using Pascal's constants.⁸ Solid IR spectra ($400\text{--}4,000\text{ cm}^{-1}$) were obtained by using potassium bromide (KBr) pellets with a Polari's FT-IR spectrometer. Electronic absorption spectra were recorded on a Shimadzu 265A spectrophotometer in solution or in solid/nujol state. Cyclic voltammograms were recorded on a Bio Analytical Systems CV-50W Voltammetric Analyzer. Cyclic voltammetric measurements were made with a three electrode system. The reference electrode was Ag/Ag^+ (0.01 M $\text{AgNO}_3/0.1$ M TEAP CH_3CN solution) electrode. The working electrode used for cyclic voltammetry was a platinum electrode, and the auxiliary electrode was a small piece of platinum wire. The solutions used for all techniques were consisted of 0.1 M tetraethylammonium perchlorate (TEAP) as supporting electrolyte in *N,N*-dimethylformamide and metal complex concentration of $10^{-3}\text{--}10^{-4}$ M scale.

Results and Discussion

The *d.c* powdered electrical conductivities (σ_H) were determined by compressing the bulk sample between two graphite rods using the two electrode system connected with potentiostat at room temperature. The results of the electrical conductivities of TTF-metal compounds are given in Table 1. The electrical conductivities of $(\text{TTF})\text{OsCl}_4 \cdot 1/2\text{C}_2\text{H}_5\text{OH}$ is up to the range of insulator, whereas the other compounds are in the range of semiconductor. This result is responsible for the fact that TTF in $(\text{TTF})\text{OsCl}_4 \cdot 1/2\text{C}_2\text{H}_5\text{OH}$ are fully ionized TTF^{2+} , whereas TTF in $(\text{TTF})_3\text{AuCl}_2$, $(\text{TTF})_{3.5}\text{AuCl}_2$, $(\text{TTF})_3\text{PtCl}_4$ and $(\text{TTF})_2\text{IrCl}_4$ compounds are partially ionized to give complex charge transfer salts. Additional evidences for stacks of TTF radicals are provided by the magnetic and spectroscopic investigations described in the following sections.

The EPR spectra were obtained for powdered samples at 77 K. The results are also given in Table 1. The EPR spectrum of a powdered sample of $(\text{TTF})_3\text{AuCl}_2$ at 77 K exhibits

Table 1. EPR parameters and magnetic properties of powder sample $(\text{TTF})_n\text{MCl}_m$ compounds

Compound	σ_H (S cm^{-1})	EPR parameters		Magnetic moment ^c (BM)
		<i>g</i> value ^a	linewidth ^b (Gauss)	
$(\text{TTF})_3\text{AuCl}_2$	4.53×10^{-3}	$g_{\parallel} = 2.0029$ $g_{\perp} = 2.0081$	5	0.86
$(\text{TTF})_{3.5}\text{AuCl}_2$	6.37×10^{-3}	$g_{\parallel} = 2.0025$ $g_{\perp} = 2.0084$	5	0.91
$(\text{TTF})_3\text{PtCl}_4$	5.51×10^{-4}	$\langle g \rangle = 2.0073$	9	0.94
$(\text{TTF})_2\text{IrCl}_4$	2.40×10^{-5}	$\langle g \rangle = 2.0080$	17	0.82
$(\text{TTF})\text{OsCl}_4 \cdot 1/2\text{C}_2\text{H}_5\text{OH}$	4.46×10^{-7}	$\langle g \rangle = 2.0069$	21	0.73

^aThe listed *g* values were measured at 77 K. ^bThe values are peak-to-peak linewidth (ΔH_{pp}). ^cThe magnetic moments were measured at room temperature.

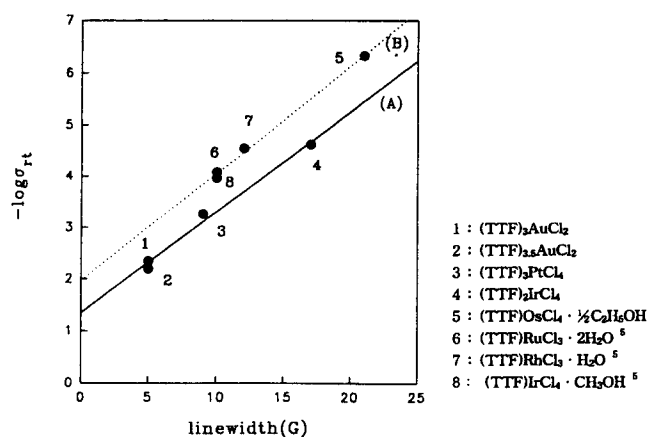


Figure 1. The plot of $-\log\sigma_0$ vs. EPR linewidth (ΔH_{pp}) for $(\text{TTF})_n\text{MCl}_n$ compounds.

an unsymmetrical shaped spectrum with $g_{\parallel}=2.0029$ and $g_{\perp}=2.0081$. $(\text{TTF})_2\text{IrCl}_4$ gave a symmetrical shaped spectrum at $\langle g \rangle=2.0080$. This value is nearly equal to the value of TTF radical in solution ($g=2.00838$)⁹ and to the values observed for a selection of salts containing the TTF donor which shows $g=2.0073$ - 2.0081 .¹⁰ The EPR spectra of $(\text{TTF})_3\text{PtCl}_4$ and $(\text{TTF})\text{OsCl}_4 \cdot 1/2\text{C}_2\text{H}_5\text{OH}$ compounds were also observed symmetrical shaped spectra. The observed g values indicate that the EPR signals are arisen from unpaired electrons distributed on TTF. These values are also comparable to those of $(\text{TTF})_4\text{CuCl}_2$ and $(\text{TTF})_4\text{CuBr}_2$ which the odd electron resides on TTF stacks. The EPR signals attributed to metal ions were not detected in the spectra, implying that the metal atoms are diamagnetic; low-spin Au(I) d^{10} , Pt(II) d^8 , Ir(III) d^6 , and Os(II) d^6 .

The linewidth can be used as a measure of the deviation of a system from one dimensionality. The observed linewidths of TTF-Au, -Pt, -Ir, and -Os compounds at 77 K are 5-21G values which are comparable to those of $(\text{TTF})_{11}(\text{SCN})_6$ ($\sim 11\text{G}$)^{10,11} and $(\text{TTF})_{11}(\text{SeCN})_6$ ($\sim 15\text{G}$).¹⁰ These relatively small values are considered as the significant interaction along the low-dimensional TTF stacks. Tomkiewicz and Taranko¹² have explained the variation of the interstack coupling, where it was concluded that the smaller the linewidth, the larger the coupling among the TTF stacks, thereby leading to the better conductivity in the stacking direction. This is not surprising because both the conductivity and the EPR linewidth are determined by the electron-phonon scattering rate.¹³ Another example for narrow EPR lines is (fluoranthenyl)₂SbF₆,¹⁴ in which the narrow linewidths are effected from the delocalization of the electrons over the fluoranthenyl stacks. In order to understand the relation of electrical conductivity and EPR linewidth, we plot the $-\log\sigma_0$ versus EPR linewidth (ΔH_{pp}) in Figure 1. As EPR linewidth decreases, the electrical conductivity ($\log\sigma_0$) increases, showing good linear relationship in partially oxidized TTF compounds with Au, Pt and Ir chlorides (line A), whereas $(\text{TTF})\text{OsCl}_4 \cdot 1/2\text{C}_2\text{H}_5\text{OH}$ deviates from this line. This deviation is expected to be arisen from complete charge of TTF in $(\text{TTF})\text{OsCl}_4 \cdot 1/2\text{C}_2\text{H}_5\text{OH}$. However, $(\text{TTF})\text{OsCl}_4 \cdot 1/2\text{C}_2\text{H}_5\text{OH}$ shows good linear relationship with Ru, Rh-compounds which contain completely charged TTF (line B). These results show that the elect-

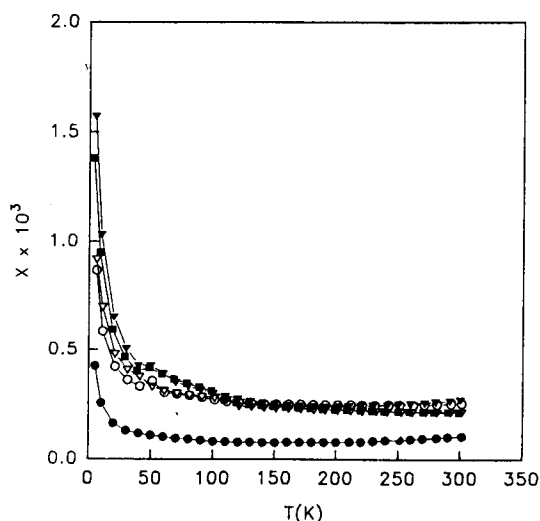


Figure 2. Temperature dependence of magnetic susceptibility for $(\text{TTF})_n\text{MCl}_n$ compounds. ● $(\text{TTF})_3\text{AuCl}_2$; ○ $(\text{TTF})_{3.5}\text{AuCl}_2$; ▼ $(\text{TTF})_3\text{PtCl}_4$; ■ $(\text{TTF})_2\text{IrCl}_4$; △ $(\text{TTF})\text{OsCl}_4 \cdot 1/2\text{C}_2\text{H}_5\text{OH}$.

rical conductivity is affected both by the EPR linewidth expressed low-dimensionality and by the degree of charge on TTF.

The temperature dependences of the magnetic susceptibilities for the prepared compounds from 4 to 300 K are shown in Figure 2. The magnetic susceptibilities increase very slightly as the temperature decreases, and increase sharply at low temperature as Curie-like tail, but the data are not described by the Curie law $\chi(T)=C/T$. However, the temperature dependence of the magnetic susceptibilities is rather weaker than in Curie law. This weak temperature dependence is responsible for the fact that the unpaired electrons are delocalized extensively over TTF spin lattices. The effective magnetic moments (μ_{eff}) arisen from this delocalized electron are 0.73-0.94 B.M, which are somewhat less than the spin-only value of 1.73 B.M for one unpaired electron. This observation, together with the results of EPR spectra, is consistent with the conclusion that the oxidation states of metal ions are diamagnetic Au(I) d^{10} , Pt(II) d^8 , Ir(III) d^6 , and Os(II) d^6 state, and that the unpaired electrons are delocalized over the $(\text{TTF})_n^+$ radicals.

The IR spectra were obtained by using KBr pellets. All of the TTF-metal chloride compounds showed a very broad intense band extending from the near IR region to a band edge at *ca.* 1200 cm^{-1} . The intense absorptions are arisen from the band structure of the semiconductors and masked many of the vibrational modes of the compounds. Such effects are commonly observed in highly conductive charge transfer salts.¹⁵ A limited number of vibrational bands of TTF in the TTF-metal chloride salts are found in the absorption tail in the range of 400 - 1400 cm^{-1} . The vibrational modes are tentatively assigned by comparing their positions and intensities with the reported spectra of one-dimensional TTF compounds.⁹ The spectral bands and their assignments are listed in Table 2. The IR assignments have been made for TTF^+ ions as well as for TTF molecule.¹⁶ The band observed at *ca.* 824 cm^{-1} in the spectrum of $(\text{TTF})_3\text{AuCl}_2$ can be assigned to the ν_{16} mode (CS stretch) and the ν_{25} band (ring

Table 2. Selected ν_{15} , ν_{16} , ν_{25} , and ν_{14} vibrational modes of $(\text{TTF})_m\text{MCl}_n$ compounds

Compound	Absorption Maxima (cm^{-1})			
	ν_{15}	ν_{16}	ν_{25}	ν_{14}
TTF ⁰ ^a	1095	781	794	1530
TTF ⁺ ^a	1072	836	825	1478
$(\text{TTF})_3\text{AuCl}_2$	1084	824	816	1501
$(\text{TTF})_{3.5}\text{AuCl}_2$	1082	825	810	1500
$(\text{TTF})_3\text{PtCl}_4$	1095	824	809	1500
$(\text{TTF})_2\text{IrCl}_4$	1086	832	822	1494
$(\text{TTF})\text{OsCl}_4 \cdot 1/2\text{C}_2\text{H}_5\text{OH}$	1089	862	802	1451
$(\text{TTF}^{2+})(\text{BF}_4^-)_2$ ^b				1440

^a reference 9. ^b reference 18**Table 3.** Electronic absorption wavelengths of $(\text{TTF})_m\text{MCl}_n$ compounds

Compound	Electronic spectra	
	λ_{max}	Solvent
$(\text{TTF})_3\text{AuCl}_2$	232, 317, 441, 586	DMF
	215, 311, 384, 582	solid/nujol
$(\text{TTF})_{3.5}\text{AuCl}_2$	261, 316, 442, 586	DMF
	226, 301, 365, 567	solid/nujol
$(\text{TTF})_3\text{PtCl}_4$	226, 305, 439, 564	DMF
	220, 288, 362, 550	solid/nujol
$(\text{TTF})_2\text{IrCl}_4$	265, 319, 363, 530	DMF
	220, 298, 364, 523	solid/nujol
$(\text{TTF})\text{OsCl}_4 \cdot 1/2\text{C}_2\text{H}_5\text{OH}$	257, 317, 374, 562	DMF
	222, 329, 402, 546	solid/nujol

SCC bend) is generally masked by the ν_{16} band. A shoulder observed at 816 cm^{-1} in the spectrum of $(\text{TTF})_3\text{AuCl}_2$ may be assigned to the ν_{25} mode. Both the C-S band (ν_{16}) and C=C band (ν_{15}) are usually affected by the variation of bond orders and bond lengths due to the oxidation of TTF. The observed values are between those reported to the TTF molecules (ν_{15} : 1095, ν_{16} : 781 cm^{-1}) and the TTF from radical (ν_{15} : 1072, ν_{16} : 836 cm^{-1}), providing further evidence of the partial oxidation of the TTF molecule in $(\text{TTF})_3\text{AuCl}_2$ compound (ν_{15} : 1082, ν_{16} : 824 cm^{-1}). Similar results were observed for the $(\text{TTF})_3\text{PtCl}_4$ and $(\text{TTF})_2\text{IrCl}_4$ compounds. Whereas the observed value of ν_{14} (C=C stretching bands) in $(\text{TTF})\text{OsCl}_4 \cdot 1/2\text{C}_2\text{H}_5\text{OH}$ compound is close to that in $(\text{TTF}^{2+})(\text{BF}_4^-)_2$ salt.¹⁷ Of the C-C stretching bands in five membered TTF ring, the ν_{14} mode has been observed to undergo large shifts of approximately 50 cm^{-1} per unit charge on oxidation of TTF.¹⁸ Therefore the observed ν_{14} value indicates that $(\text{TTF})\text{OsCl}_4 \cdot 1/2\text{C}_2\text{H}_5\text{OH}$ consists of TTF^{2+} and OsCl_4^{2-} .

Electronic spectra were recorded from 200-800 nm both in DMF solution and solid/nujol state. The results are summarized in Table 3. Wudl et al.⁹ have reported the maximum absorbance wavelength (λ_{max}) of the TTF radical in H_2O appears at 340 ($b_{3g} \rightarrow b_{1u}$), 435 ($b_{1u} \rightarrow b_{2g}$), and 575 nm ($b_{2g} \rightarrow b_{1u}$). These electronic transitions are comparable to the results found for the compounds in this study. The absorption bands

above 500 nm is interpreted as the intramolecular interaction of conjugated π molecular radicals.¹⁸

Cyclic voltammograms of TTF-metal compounds were recorded in DMF/0.10 M TEAP from -1.6 to $+0.8$ V versus a Ag/Ag^+ (0.01 M AgNO_3 /0.1 M TEAP CH_3CN solution) electrode. The cyclic voltammogram of $(\text{TTF})_3\text{AuCl}_2$ shows $E_{1/2}$ potentials at -0.01 V ($E_{pc} = -0.04$, $E_{pa} = 0.05$ V) for the TTF/TTF⁺ couple and at $+0.23$ V ($E_{pc} = 0.20$, $E_{pa} = 0.25$ V) for the TTF⁺/TTF²⁺ couple. The cyclic voltammogram of TTF also exhibits almost same values: one at ~ 0 V and the other at $+0.23$ V. Similar results were observed for the other TTF-Pt, Ir, and Os chlorides compounds. A peak attributable to metal was not detected in any case, and hence oxidation-reduction of the complex is localized to the ligands rather than to the metal center.¹⁹

Conclusions

We have prepared $(\text{TTF})_3\text{AuCl}_2$, $(\text{TTF})_{3.5}\text{AuCl}_2$, $(\text{TTF})_3\text{PtCl}_4$, $(\text{TTF})_2\text{IrCl}_4$, and $(\text{TTF})\text{OsCl}_4 \cdot 1/2\text{C}_2\text{H}_5\text{OH}$ charge transfer compounds from the reaction of TTF and the corresponding hydrogen metal chlorides. The experimental results show that incomplete charge transfer has occurred from TTF donor to gold, platinum and iridium respectively, whereas $(\text{TTF})\text{OsCl}_4 \cdot 1/2\text{C}_2\text{H}_5\text{OH}$ has completely ionized TTF²⁺ ion in a form of simple salt. The odd electrons are extensively delocalized over the TTF lattice in each compound. This low-dimensional interstack interaction is reflected in the electrical and EPR parameters. The smaller EPR linewidth, the better electrical conductivity in both the partially and completely ionized TTF charge transfer compounds. This observation may be useful in the design of molecular based conducting materials with prescribed electrical and EPR properties.

Acknowledgment. This work was supported by Il-Ju Scholarship and Culture Foundation (1995) and by Basic Science Research Program, Ministry of Education, KOREA (BSRI-95-3410).

References

- Hatfield, W. E. *Molecular Metals*; NATO Conference Series, Plenum: New York, 1979.
- Coleman, L. G.; Cohen, M. J.; Sandman, D. J.; Yamagishi, F. G.; Garito, A. F.; Heeger, A. J. *Solid State Commun.* **1973**, *12*, 1125.
- Ferraris, J.; Cowan, D. O.; Valatka, V.; Perstein, Jr., J. H. *J. Am. Chem. Soc.* **1973**, *95*, 948.
- Torrance, J. B. *Acc. Chem. Res.* **1979**, *12*, 79.
- Kim, Y. I.; Hatfield, W. E. *Inorganica Chimica Acta.* **1991**, *188*, 15.
- Kim, Y. I.; Choi, S. N.; Jung, W. S. *Bull. Korean Chem. Soc.* **1994**, *15*, 465.
- Moon, S. B.; Moon, J. D. *Bull. Korean Chem. Soc.* **1994**, *15*, 1042.
- Konig, E. *Magnetic Properties of Coordination and Organometallic Transition Metal Complexes*; Springer, Berlin, 1966.
- Wudl, F.; Smith, G. M.; Hufnagel, E. J. *J. Chem. Soc., Chem Commun.* **1970**, 1453.
- Carara, L.; Gerson, F.; Cowan, D. O.; Lerstrup, K. *Helv. Chim. Acta.* **1985**, *97*, 201.

11. Tomkiewicz, Y.; Engler, E. M. *Bull. Am. Phys. Soc. B* **1975**, *20*, 479.
12. Tomkiewicz, Y.; Taranko, A. R. *Phys. Rev. B* **1978**, *18*, 733.
13. Tomkiewicz, Y. *EPR of Organic Conductor*; in *The Physics and Chemistry of Low Dimensional Solids*; by Alcacer. D. Reidel Pub. Comp. NATO Advanced Study Institute Series, 1980.
14. Mehring, M.; Spengler, J. *Phys. Rev. Lett.* **1984**, *53*, 2441.
15. Wheland, R. C.; Gillson, J. L. *Am. Chem. Soc.* **1976**, *98*, 3916.
16. Bozio, R.; Gilando, A.; Pecile, C. *Chem. Phys. Lett.* **1977**, *52*, 503.
17. Seidle, A. R.; Candela, T. F.; Finnegan, T. F.; Van Duyne, R. P.; Cape, T.; Kokoszka, G. F.; Woyciejes, P. M.; Hashmall, J. A. *Inorg. Chem.* **1981**, *20*, 2635.
18. Torrance, J. B.; Scott, B. A.; Welber, B.; Kaufman, F. B.; Seiden, P. E. *Phys. Rev. B.* **1979**, *19*, 730.
19. Bonai, R. D. R.; Brian, B. E.; Michael, A. H. *Inorganica Chimica Acta.* **1986**, *119*, 195.

Dissociative Recombination Rates of O_2^+ Ion with Low Energy Electrons

Jeonghee Seong and Hosung Sun*

*Department of Chemistry, Pusan National University, Pusan 609-735 and
Center for Molecular Science, KAIST, Taejeon 305-701, Korea*

Received August 21, 1996

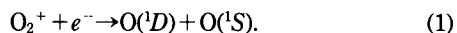
The dissociative recombination of $O_2^+(v^+) + e^- \rightarrow O(^1S) + O(^1D)$ has been theoretically investigated using the multichannel quantum defect theory (MQDT). Cross sections and rate coefficients at various electron energies are calculated. The resonant structures in cross section profile, which are hardly measurable in experiments, are also determined and the existence of Rydberg states is found to affect the rates. The theoretical rate coefficients are computed to be smaller than experimental ones. The reasons for this difference are explained. The two-step MQDT procedure is found to be very useful and promising in calculating the state-to-state rates of the dissociative recombination reaction which is a very important and frequently found phenomenon in Earth's ionosphere.

Introduction

The capture of an electron by a positive ion (recombination) requires that the electron goes from a free to a bound state and thus, in some manner, gives off energy. The energy may be given to a third body or it may be radiated away as a result of free-bound transition. When the third body is the molecule (the positive ion combined with the incident electron) itself, the releasing energy can break the molecule into atomic fragments. This phenomenon is called dissociative recombination of an ion with an electron.

The green line of oxygen is observed in the night sky and in aurora. It was suggested that the oxygen green line which is a prominent feature of the spectrum of the night sky is due to the formation of the excited atom $O(^1S)$ through the dissociative recombination of O_2^+ ions with electrons¹.

The following reaction produces the oxygen atom in the excited 1S state



And, in the upper atmosphere, this $O(^1S)$ falls into the lower 1D state and, consequently, the light of 5577 Å (green) is emitted.² Therefore, in astrophysics, it is of considerable interest to determine the recombination rates for production of excited oxygen atoms.

Zipf has measured the absolute intensities of $^1S(5577 \text{ Å})$ and $^1D(6300 \text{ Å})$ radiation coming out from the reaction (1) using a microwave afterglow apparatus.³ By relating the decay of intensity to the measured decay of electron density, he obtained values for the partial rates; namely, $\alpha(^1S) = 2.1 \times 10^{-9} \text{ cm}^3/\text{sec}$ and $\alpha(^1D) = 1.9 \times 10^{-7} \text{ cm}^3/\text{sec}$ at 300 K. And his microwave afterglow results gave a quantum yield of 0.1 and 0.9 for $O(^1S)$ and $O(^1D)$, respectively.

During the last decade, in both laboratory and *in situ* atmospheric experiments the quantum yield of the excited states $O(^1S)$, $O(^1D)$, and $O(^1P)$ of oxygen atoms was explored.⁴⁻¹¹ And a review for the $O(^1S)$ quantum yields obtained from the satellite and rocket measurements was given by Yee *et al.*¹² Since the total rate as a function of ion vibrational level (v^+) has not been determined experimentally, the theoretical quantum yields for $v^+ = 1$ and 2 can test the assumption that the total rate is constant over v^+ .

From a theoretical point of view, the dissociative recombination can be considered as an ion-electron collision process. So dynamic theories can be applied to this problem. Among those theoretical tools, multichannel quantum defect theory (MQDT) has been successful in investigating dissociative recombinations of H_2^+ ,¹³⁻¹⁹ HD^+ ,¹⁹ D_2^+ ,^{19,20} CH^+ ,²¹ and NO^+ ions²²⁻²⁷ with low energy electrons.

MQDT²⁸⁻³⁰ has brought a remarkable progress to theoretic-